

# Lab on a Chip

Accepted Manuscript



This is an *Accepted Manuscript*, which has been through the Royal Society of Chemistry peer review process and has been accepted for publication.

*Accepted Manuscripts* are published online shortly after acceptance, before technical editing, formatting and proof reading. Using this free service, authors can make their results available to the community, in citable form, before we publish the edited article. We will replace this *Accepted Manuscript* with the edited and formatted *Advance Article* as soon as it is available.

You can find more information about *Accepted Manuscripts* in the [Information for Authors](#).

Please note that technical editing may introduce minor changes to the text and/or graphics, which may alter content. The journal's standard [Terms & Conditions](#) and the [Ethical guidelines](#) still apply. In no event shall the Royal Society of Chemistry be held responsible for any errors or omissions in this *Accepted Manuscript* or any consequences arising from the use of any information it contains.

## COMMUNICATION

# A Microsystem Integrating Photodegradable Hydrogel Microstructures and Reconfigurable Microfluidics for Single Cell Analysis and Retrieval

Cite this: DOI: 10.1039/x0xx00000x

Received 00th January 2012,  
Accepted 00th January 2012

Kyung Jin Son, Dong-Sik Shin, Timothy Kwa, Jungmok You, Yandong Gao and Alexander Revzin\*

DOI: 10.1039/x0xx00000x

[www.rsc.org/](http://www.rsc.org/)

**We developed a micropatterned photodegradable hydrogel array integrated with reconfigurable microfluidics to enable cell secretion analysis and cell retrieval at the single cell level. Activity of protease molecules secreted from single cells was monitored using FRET peptides entrapped inside microfabricated compartments. Antibody-modified gel islands tethering cells to the surface could be degraded by UV exposure to release specific single cells of interest.**

Cell populations often exhibit heterogeneity<sup>1,2</sup> in the phenotypic and functional characteristics, such as cell morphology and proliferation<sup>3,4</sup>, response to external stimuli<sup>5,6</sup> and protein secretory activities<sup>7-10</sup>. Much of the current understanding of cell function is based on population-averaged assays which do not provide information about individual cells<sup>11</sup> and may mask the presence of subpopulations of cells showing distinct behaviors<sup>12</sup>. Therefore, single cell analysis is important to elucidate phenotypic heterogeneity among cells. Recent developments in microtechnologies including microwells<sup>13</sup>, microtubes<sup>14</sup>, micropallets<sup>15</sup>, and microtraps<sup>16</sup> allow capture and analysis of single cells. These approaches are valuable for single cell analysis; however, retrieval of single cells of interest remains challenging. Electrochemical release from electrodes<sup>17, 18</sup>, physicochemical stimulation<sup>19</sup>, and micromanipulators<sup>20</sup> have been used, but these methods often threaten cell viability due to physiologically unfavorable conditions or cell damage by direct contact.

Release of proteins from cells may correlate with pathological developments and may be used for disease diagnosis. Because of this, there is significant interest in analyzing secretions of proteins including cytokines<sup>8, 10, 21</sup>, antibodies<sup>22, 23</sup> and proteases<sup>24</sup> at the single cell level. Matrix metalloproteinases (MMPs) are one class of proteases that have received significant attention as important

biomarkers of cancer diagnosis and treatment. For example, MMP9 degrades the basement membrane of extracellular matrix (ECM), facilitating cancer cell invasion and metastasis.<sup>25, 26</sup> Our lab has recently described the use of fluorescence resonance energy transfer (FRET)-based peptides, specific to MMP9 as well as MMP2, to monitor protease release from small groups of cells<sup>27</sup>. Herein, we wanted to extend detection to single cells. In addition, it may be important to complement detection of single cell secretions with the ability to retrieve specific cells based on secreted factors. In an effort to enable function-based cell sorting, our laboratory has developed photodegradable hydrogels that can be fabricated into microstructures and can be functionalized with cell-adhesive ligands<sup>28, 29</sup>. In the present paper, we describe a microsystem that allows to capture and confine single cells in high-density arrays of microcompartments in order to detect protease secretion from single cells. Because single cells are captured on photodegradable hydrogel islands, they can be released by light-induced degradation of the gel. Using this microsystem it was possible to analyze protease secretion dynamics from 500 single cells and to release specific cells from the surface.

An array of photogel islands was prepared on glass slides, then modified with CD4 antibodies (Abs), and integrated with a reconfigurable microfluidic (see Supporting Information for experimental details). As seen in Fig. 1A, an individual microchamber contained a photogel island (diameter = 20  $\mu\text{m}$ ) for single cell capture and release. For cell capture, lymphoma cells (U-937 cells;  $2 \times 10^6$  cells  $\text{mL}^{-1}$ ) in serum-free and Phenol Red-free RPMI-1640 media (working media) were infused into the channel at  $2.5 \mu\text{L min}^{-1}$  for 20 min. Unbound cells were removed by washing with working media at  $10 \mu\text{L min}^{-1}$  for 10 min. For detection of secretory activity, a solution containing FRET peptides (40 nM; Gly-Pro-Leu-Gly-Met-Trp-Ser-Arg-Glu-Cys, GL Biochem) and mitogen (100 ng  $\text{mL}^{-1}$  PMA) in working media was infused into the channel at  $10 \mu\text{L min}^{-1}$  for 15 min, after which the microfluidic device was

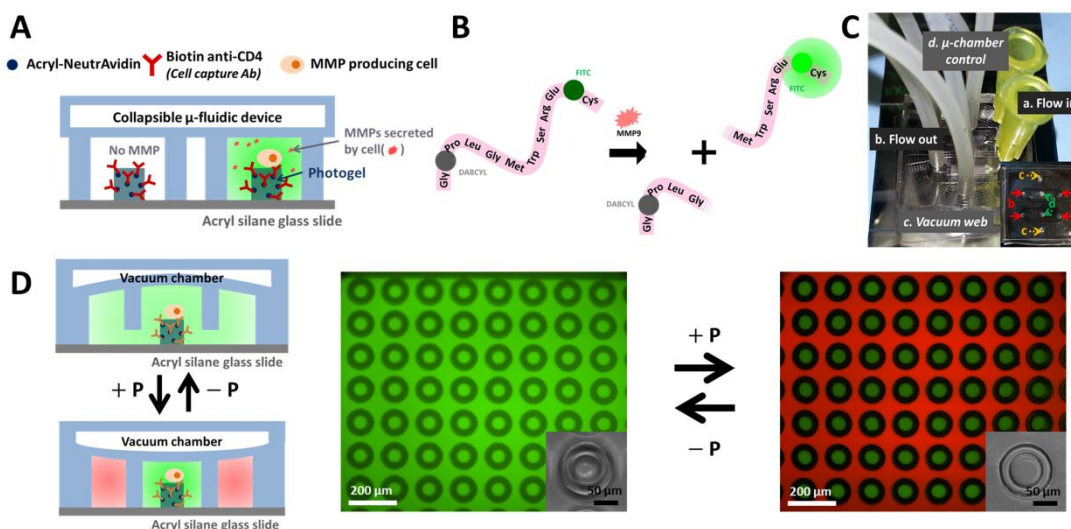


**Fig. 1** (A) Individual microchamber consisting of a photogel island with CD4 antibodies for cell capture surrounded by free floating protease sensing FRET-peptides. (B) Design of MMP9 sensing peptide with cleavage site between Gly and Met. (C-D) Design of a reconfigurable microfluidic device for high-throughput and ultrasensitive protease detection. (C) Photographs of device and (D) microscope images showing working principle using red/green fluorophores (Atto 594-Biotin/FITC-BSA) and verifying complete isolation of individual microchambers.

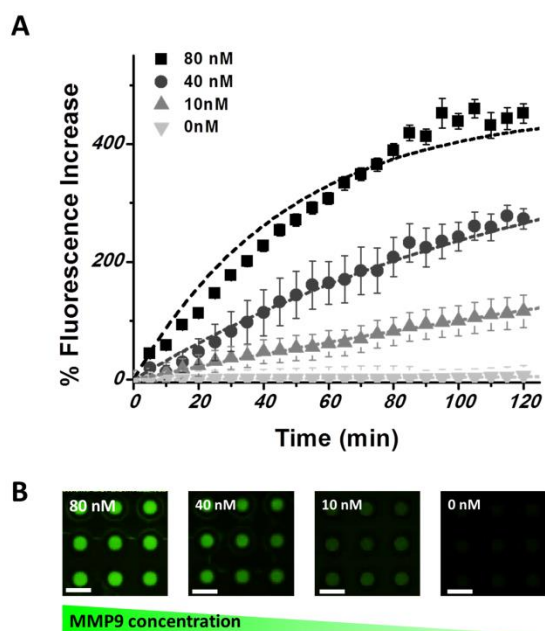


**Fig. 2** Fluorescence detection of recombinant MMP9 and modeling of peptide cleavage. (A) Comparison of experimental data (dots) and simulation results (dotted lines): Responses of free floating sensing FRET-peptides to varying MMP9 concentrations over time. (B) Fluorescence images of FRET-peptides challenged with different MMP9 concentrations after 120 min of incubation. Scale bar: 200 $\mu$ m.

**Table 1. Michaelis – Menten Kinetics Variables for MMP9 Proteases**

$K_M$	210.17 nM
$k_{cat}$	0.0551 min <sup>-1</sup>

reconfigured to create an array of discrete microchambers. These peptides, described by us in a recent report<sup>27</sup>, are designed to contain donor/acceptor FRET pair (FITC and DABCYL) and are cleaved by MMP9 or MMP2 (Fig. 1B). After the cleavage, the distance between donor and acceptor chromophore increases and signal comes on. The signal was monitored using fluorescence microscopy with microchambers placed inside a custom built environmental chamber (37°C under 5% CO<sub>2</sub> atmosphere). Time-lapse images were acquired at 10 min intervals for a total of 2 h.

Fig 1(C,D) demonstrate set-up and operation of reconfigurable microfluidic devices. As shown in Fig. 1D, the flow layer is raised by applying vacuum to the control channel; allowing green fluorophore-labeled protein solution (FITC-BSA, 1 mg mL<sup>-1</sup>, Sigma) to be distributed uniformly throughout the channel. Releasing the vacuum, causes the roof of the microfluidic device with engraved microcups (diameter = 60  $\mu$ m, height = 50  $\mu$ m) to descend onto the floor of the device, confining photogel islands inside ~140 pL chambers. The green fluorophore remaining outside microchambers was washed and replaced by red fluorophore (Atto 594-biotin, 0.1 mg mL<sup>-1</sup>, Sigma). Fig. 1D shows that microcups with green fluorescent molecules are isolated from each other and are distinct from the interstitial space containing red fluorescence molecules. This experiment was designed to highlight that crosstalk between adjacent chambers did not occur and that individual cells were effectively sequestered using reconfigurable microfluidic device.

For calibration purposes, FRET-peptides were mixed with various concentrations of recombinant MMP9 (human; 0 – 80 nM; Sigma Aldrich) in working media at 37 °C and infused into microfluidic devices (Fig. 2). Peptide cleavage by MMP9 was monitored for 2 h using Nikon eclipse Ti fluorescence microscope with 480 $\pm$ 20nm/ 535 $\pm$ 25 nm excitation/emission filters and analysis of acquired fluorescence images was carried out using AxioVision software. The limit of detection was determined to be 2.3 nM based on signal-to-noise characteristics (S/N = 3)<sup>30</sup> at t = 120 min, while the linear range extended to 80 nM<sup>31</sup>.

To determine MMP9 secretion rates of single cells, parameters associated with enzymatic activity of MMP9 were obtained, and then, incorporated into a diffusion-reaction model (see Supporting

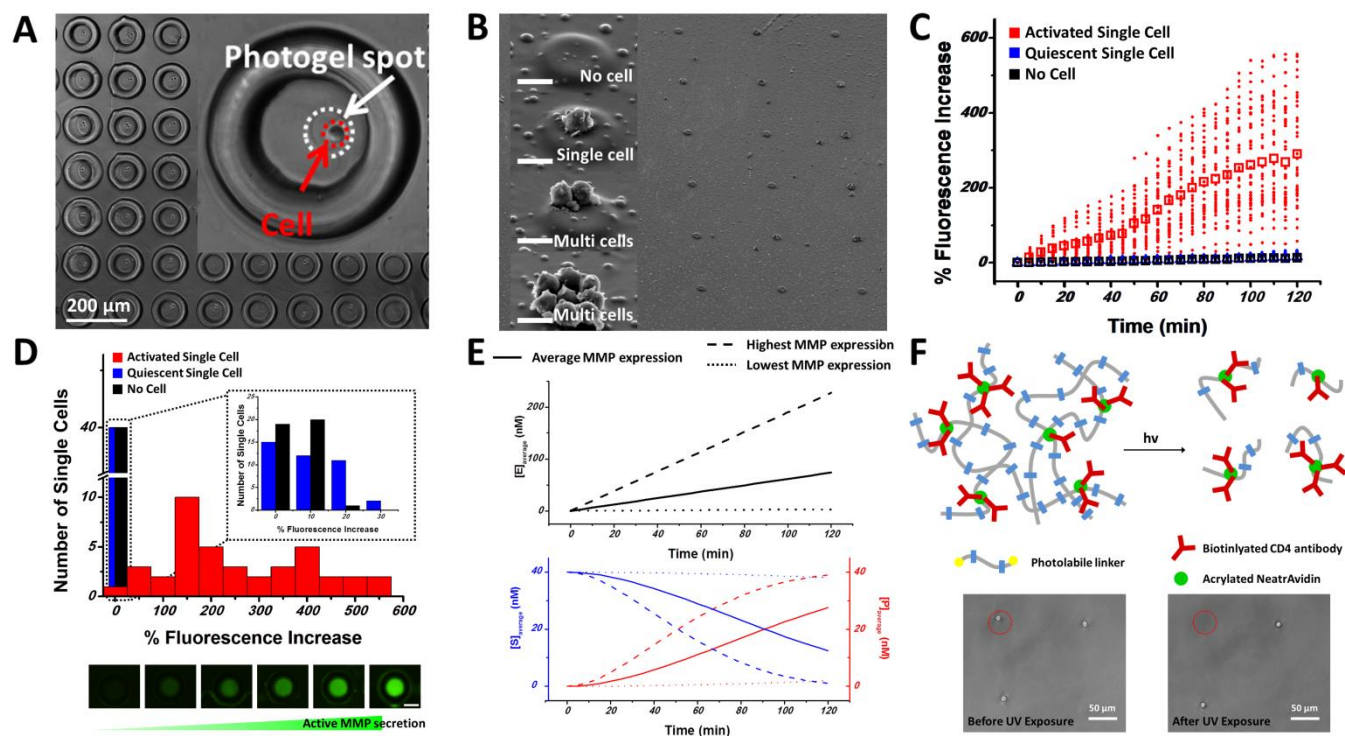


**Fig. 3** (A-B) CD4 Ab-modified photogel islands for selective cell capture and release: this photogel island (diameter = 20  $\mu\text{m}$ ) could capture  $1 \pm 1$  cells ( $n = 558$ ). (A) Optic and (B) scanning electron microscope images of U-937 cells captured mostly on top of Ab-containing photogel islands. (C-D) Monitoring proteolytic activities of MMP9 secreted from single cells. Scale bar = 10  $\mu\text{m}$ . (C) Change in fluorescence of free floating FRET-peptides for microwells with mitogenically activated single cells (red), quiescent single cells (blue) and no cells (black) ( $n = 40$  for each group). (D) Heterogeneity of activated single U-937 cells in producing MMP9. (E) Numerical simulation results showing the average concentration profile of MMP9, FRET-peptides, and cleaved peptides over time for activated single cells. Scale bar = 50  $\mu\text{m}$ . (F) Selective cell retrieval via photodegradation of photogel islands: schematics illustrating the degradation of photogel under UV irradiation and optic images showing the selective retrieval of high MMP expressing single cell.

Information for details). By fitting experimental data (dots in Fig. 2A) to the Schnell-Mendoza equation<sup>32</sup> using MATLAB, catalytic constant ( $k_{cat}$ ) and Michaelis – Menten constant ( $K_m$ ) were determined to be  $0.0551 \text{ min}^{-1}$  and 210.17 nM, respectively. The specificity constant ( $k_{cat}/K_m$ ) for free floating FRET-peptide GPLGMWSRKC was  $0.44 \times 10^4 \text{ M}^{-1}\text{s}^{-1}$ . This is comparable to the value of  $0.8 \times 10^4 \text{ M}^{-1}\text{s}^{-1}$  for an immobilized FRET-peptide GPLGMWSRKC determined in the previous paper.<sup>27</sup>

Finally, the possibility of monitoring production of MMP9 by single cells in our microsystems was demonstrated. The number of cells bound a photogel island depends on cell concentration as well as flow rate of cell suspension during seeding. Fig. 3A-B, shows U937 cell capture under optimized conditions of  $2 \times 10^6 \text{ cells mL}^{-1}$  seeded at a flow rate of  $2.5 \mu\text{L min}^{-1}$  for 20 min. These conditions resulted in 37.5% single cell and 25% multi-cell capture on 20  $\mu\text{m}$  diameter photogel islands.

Once cells were seeded and captured on micropatterned surfaces, peptide beacons were infused and subsequently microfluidic devices were reconfigured by lowering microcompartments onto photogel islands and captured cells. Fluorescence due to cleavage of MMP9-sensing peptides was analyzed over the course of 2h for microcompartments with activated single cells, quiescent single cells and no cells (Fig. 3C-D and S1-2, ESI). Fig. 3C shows that, on average, activated single cells produced significantly higher level of MMP9 compared to quiescent single cells. However, it is of note that only 12.5% of activated single cell generated the signal corresponding to average value (Fig. 3D). This underscores

heterogeneity in cellular production of MMP9. Importantly, LIVE/DEAD staining of cells sequestered inside microcompartments revealed viability of  $\sim 96\%$  - suggesting that confinement did not adversely affect cell survival for the 2h hour experiment (see Figure S3). In light of viability data, heterogeneity in protease secretion/activity observed in Figure 3C-D should be attributed to differences in function of single cells.

In order to convert fluorescence signals inside the microchambers into concentration profiles of MMP9 (E), FRET-peptides (S), and cleaved peptides (P), diffusion-reaction equations incorporating Michaelis-Menten and catalytic constants determined previously were solved using COMSOL Multiphysics (see Supporting Information). Results of modeling presented in Fig. S4 demonstrate that activated single cells released MMP9 at an average rate of  $0.48 \text{ pg h}^{-1}$  (RMS deviation = 9.8%), which is comparable to the value of  $0.57 \text{ pg h}^{-1} \text{ cell}^{-1}$  (for small groups of cells,  $n = 24 \pm 4$ ) reported by us previously.<sup>27</sup> MMP9 secretion rates for activated single cells at the highest and lowest secretion level were determined to be  $1.48 \text{ pg h}^{-1}$  (RMS deviation = 8.2%) and  $0.02 \text{ pg h}^{-1}$  (RMS deviation = 7.5%), respectively. On the other hand, average MMP9 secretion rate of quiescent cell is  $0.015 \text{ pg h}^{-1}$  with RMS deviation of 2.4% (highest level =  $0.032 \text{ pg h}^{-1}$  with RMS deviation of 3.8%; lowest level =  $0.005 \text{ pg h}^{-1}$  with RMS deviation of 1.8%). In Fig. 3E, concentration of MMP9 produced by activated single cells increases over time, resulting in consumption of FRET-peptides and generation of cleaved peptides which correlate to the fluorescence signals (Fig. 3C). It is worth of

note that most of FRET-peptides are consumed by MMP9s for 2 h when the activated single cell is at the highest secretion level, which accounts for a plateau phase of fluorescence observed in Fig. 3C. Given that MMP9 is an important factor in cancer invasion, one may hypothesize that high producers of this protease may be more aggressive in cancer proliferation. While carrying out molecular biology experiments to test this hypothesis was beyond the scope of this technical paper, we did want to demonstrate the ability to release specific single cells after protease analysis.

This was achieved by exposure of specific photogel islands containing single cells to UV light using DAPI cut-off filter in a fluorescence microscope (45 mW cm<sup>-2</sup>, Nikon Instruments, Inc.). As shown in a cartoon of Figure 3F, exposure to UV lights was expected to degrade *o*-nitrobenzyl cross-linkers within PEG gel. The duration and intensity of exposure as well as dynamics of gel degradation were characterized in a recent paper by our lab<sup>29</sup>. Based on this optimization photogel islands were exposed to UV light for 5 min, causing the gel to degrade over the course of 1 hr at 37 °C. The microscopy image in Figure 3F proves the principle of selective degradation of photogel islands and release of cells. Importantly, there are studies demonstrating that amount of UV comparable to that used by us for gel degradation does not significantly damage DNA.<sup>33</sup> This bodes well for the possibility of carrying out molecular analysis on released cells in the future. It is also worth noting that UV degradation of the gel does not cause appreciable loss in cell viability.<sup>29</sup>

## Conclusions

This paper describes development of a microsystem for single cell secretion analysis and sorting. Micropatterned photo-degradable hydrogels are combined with reconfigurable microfluidics to enable capturing single cells in predefined locations on the surface and then rearranging the device geometry to confine single cells inside microchambers for sensitive detection of cell secretions. While inspired by the excellent microtechnologies for single cell analysis reported by Love and Heath groups<sup>13, 34</sup>, we wanted to demonstrate the ability to capture, analyze and release specific single cells. To enable this, substrates were micropatterned to contain hydrogel islands functionalized with cell-adhesive antibodies. These gel islands were also made photodegradable. To prove this concept, lymphoma (U-937) cells were captured inside the microfluidic device and were analyzed for protease production using free floating protease-cleavable FRET-peptides as beacons. The average secretion rates were determined by diffusion-reaction modeling to be 0.48 pg h<sup>-1</sup> and 0.015 pg h<sup>-1</sup> for activated and quiescent single cells, respectively. Based on protease secretion analysis, specific single cells were selectively released via photo-initiated degradation of hydrogel islands. Importantly, this retrievable method does not compromise cell viability<sup>29</sup> and may in the future be used for clonal expansion of specific single cells. Retrieved cells may also be lysed for more in-depth molecular biology analyses. Further future enhancement of this technology may come from design of multiple protease-specific peptide beacons with unique fluorescence signatures. Such an approach may be used for detecting multiple proteases from single cells.

## Acknowledgement

Financial support for this work was provided by grants from NSF. Additional funding came from "Research Investments in Science and Engineering from UC Davis".

## Notes and references

Department of Biomedical Engineering, University of California, Davis, USA. E-mail: arevzin@ucdavis.edu; Tel: +1-530-752-2383; Fax.: +1-530-754-5739

† Electronic Supplementary Information (ESI) available: Experimental details and materials. See DOI: 10.1039/c000000x/

1. S. J. Altschuler and L. F. Wu, *Cell*, 2010, **141**, 559-563.
2. M. L. Kovarik and N. L. Allbritton, *Trends Biotechnol*, 2011, **29**, 222-230.
3. Z. Guan, S. Jia, Z. Zhu, M. Zhang and C. J. Yang, *Anal Chem*, 2014, **86**, 2789-2797.
4. S. Ban, K. Ishikawa, S. Kawai, K. Koyama-Saegusa, A. Ishikawa, Y. Shimada, J. Inazawa and T. Imai, *Journal of radiation research*, 2005, **46**, 43-50.
5. S. Lopez-Verges, J. M. Milush, S. Pandey, V. A. York, J. Arakawa-Hoyt, H. Pircher, P. J. Norris, D. F. Nixon and L. L. Lanier, *Blood*, 2010, **116**, 3865-3874.
6. A. A. Cohen, N. Geva-Zatorsky, E. Eden, M. Frenkel-Morgenstern, I. Issaeva, A. Sigal, R. Milo, C. Cohen-Saidon, Y. Liron, Z. Kam, L. Cohen, T. Danon, N. Perzov and U. Alon, *Science*, 2008, **322**, 1511-1516.
7. H. Kortmann, F. Kurth, L. M. Blank, P. S. Dittrich and A. Schmid, *Lab on a chip*, 2009, **9**, 3047-3049.
8. Y. Lu, J. J. Chen, L. Mu, Q. Xue, Y. Wu, P. H. Wu, J. Li, A. O. Vortmeyer, K. Miller-Jensen, D. Wirtz and R. Fan, *Anal Chem*, 2013, **85**, 2548-2556.
9. Y. Shirasaki, M. Yamagishi, N. Suzuki, K. Izawa, A. Nakahara, J. Mizuno, S. Shoji, T. Heike, Y. Harada, R. Nishikomori and O. Ohara, *Scientific reports*, 2014, **4**, 4736.
10. V. Chokkalingam, J. Tel, F. Wimmers, X. Liu, S. Semenov, J. Thiele, C. G. Figdor and W. T. Huck, *Lab on a chip*, 2013, **13**, 4740-4744.
11. D. Di Carlo and L. P. Lee, *Anal Chem*, 2006, **78**, 7918-7925.
12. D. Di Carlo and L. P. Lee, *Anal Chem*, 2006, **78**, 7918-7925.
13. J. C. Love, J. L. Ronan, G. M. Grotenbreg, A. G. van der Veen and H. L. Ploegh, *Nature biotechnology*, 2006, **24**, 703-707.
14. E. J. Smith, S. Schulze, S. Kiravittaya, Y. F. Mei, S. Sanchez and O. G. Schmidt, *Nano Lett*, 2011, **11**, 4037-4042.
15. G. T. Salazar, Y. Wang, G. Young, M. Bachman, C. E. Sims, G. P. Li and N. L. Allbritton, *Anal Chem*, 2007, **79**, 682-687.
16. D. Di Carlo, L. Y. Wu and L. P. Lee, *Lab on a chip*, 2006, **6**, 1445-1449.
17. W. S. Yeo, M. N. Yousaf and M. Mrksich, *Journal of the American Chemical Society*, 2003, **125**, 14994-14995.
18. H. Zhu, J. Yan and A. Revzin, *Colloids and Surfaces B: Biointerfaces*, 2008, **64**, 260-268.
19. B. D. Plouffe, M. A. Brown, R. K. Iyer, M. Radisic and S. K. Murthy, *Lab on a chip*, 2009, **9**, 1507-1510.

## Journal Name

20. S. Yamamura, H. Kishi, Y. Tokimitsu, S. Kondo, R. Honda, S. R. Rao, M. Omori, E. Tamiya and A. Muraguchi, *Anal Chem*, 2005, **77**, 8050-8056.
21. H. Zhu, G. Stybayeva, J. Silangcruz, J. Yan, E. Ramanculov, S. Dandekar, M. D. George and A. Revzin, *Anal Chem*, 2009, **81**, 8150-8156.
22. M. P. Raphael, J. A. Christodoulides, J. B. Delehanty, J. P. Long and J. M. Byers, *Biophysical journal*, 2013, **105**, 602-608.
23. A. Kida, M. Iijima, T. Niimi, A. D. Maturana, N. Yoshimoto and S. Kuroda, *Anal Chem*, 2013, **85**, 1753-1759.
24. R. R. Tengyang Jing, Majid Ebrahimi Warkiani, Chwee Teck Lim, Jongyoon Han, and Chia-Hung Chen, *International Conference on Miniaturized Systems for Chemistry and Life Sciences*, 2013, 1373-1375.
25. A. F. Chambers and L. M. Matrisian, *Journal of the National Cancer Institute*, 1997, **89**, 1260-1270.
26. M. Egeblad and Z. Werb, *Nature reviews. Cancer*, 2002, **2**, 161-174.
27. K. J. Son, D. S. Shin, T. Kwa, Y. D. Gao and A. Revzin, *Anal Chem*, 2013, **85**, 11893-11901.
28. C. Siltanen, D. S. Shin, J. Sutcliffe and A. Revzin, *Angew Chem Int Edit*, 2013, **52**, 9224-9228.
29. D. S. Shin, J. You, A. Rahimian, T. Vu, C. Siltanen, A. Ehsanipour, G. Stybayeva, J. Sutcliffe and A. Revzin, *Angewandte Chemie*, 2014.
30. G. L. Long and J. D. Winefordner, *Anal Chem*, 1983, **55**, A712-&.
31. J. C. Waters, *J Cell Biol*, 2009, **185**, 1135-1148.
32. S. Schnell and C. Mendoza, *J Theor Biol*, 1997, **187**, 207-212.
33. S. Singh-Gasson, R. D. Green, Y. Yue, C. Nelson, F. Blattner, M. R. Sussman and F. Cerrina, *Nature biotechnology*, 1999, **17**, 974-978.
34. C. Ma, R. Fan, H. Ahmad, Q. Shi, B. Comin-Anduix, T. Chodon, R. C. Koya, C. C. Liu, G. A. Kwong, C. G. Radu, A. Ribas and J. R. Heath, *Nature medicine*, 2011, **17**, 738-743.